2022-04

The Effect of Navier Slip and Skin Friction on Nanofluid Flow in a Porous Pipe

Muyungi, Wivina

Engineering, Technology and Applied Science Research

https://doi.org/10.48084/etasr.4763

The Effect of Navier Slip and Skin Friction on Nanofluid Flow in a Porous Pipe

Wivina Nathan Muyungi
School of Computational and Communication Science and Engineering, Nelson Mandela African Institution of Science and Technology, Arusha, Tanzania
muyungiw@nm-aist.ac.tz

Michael Hamza Mkwizu
Department of Mathematics and Statistics
Sokoine University of Agriculture
Morogoro, Tanzania
mkwizumh@gmail.com

Verdiana Grace Masanja
School of Computational and Communication Science and Engineering
Nelson Mandela African Institution of Science and Technology
Arusha, Tanzania
verdiana.masanja@nm-aist.ac.tz

Received: 18 January 2022 | Revised: 7 February 2022 | Accepted: 11 February 2022

Abstract-The flow of nanofluids through a porous medium is considered the optimum method for convective heat transfer. In this study, nanofluid flow in a porous pipe with Navier slip is investigated. Two water-based nanofluids, Copper (Cu) and alumina (Al_2O_3), were considered. The governing equation is presented and non-dimensionalization has been done for momentum and energy equations, initial and boundary conditions, skin friction, and Nusselt number. The governing system was simplified to ordinary differential equations, which were numerically solved and a mathematical model of nanofluid flow was formulated. The results, with regard to variations in various parameters such as temperature, velocity, skin friction, and Nusselt number, are presented graphically and discussed. It was found that the velocity during the flow decreases with the increase of the Navier slip.

Keywords-Navier slip; skin friction; nanofluid; porous pipe

I. INTRODUCTION

Flow of a fluid through porous media occurs in many technical fields such as ground water flows, flow through embankment dams, composite-structures (culverts), filtering and waste water treatment. Authors in [1] studied the fluid flow in a uniform porous pipe considering suction and injection. They established that changes of velocity and vorticity were great in the boundary layer while outside the boundary layer their variation is low. Authors in [2] investigated the flow of nanofluids in porous media and the influence of the flow on heat transfer. It was discovered that porous media and nanofluids can be used to improve heat transmission. Although the flowing of fluids through porous media has been a subject of great interest for centuries, however, recently, the movement of nanofluids in porous media has caught a lot of attention especially in cooling systems, filtering systems, heat transfer, diffusion, and osmosis.

In 1995, authors in [3] introduced new coolant fluids called nanofluids which, when compared to pure liquids exhibit the following advantages: higher specific surface area, greater dispersion stability with predominantly Brownian particle motion, reduced pumping power to obtain an equivalent intensity of thermal transfer, and reduction of the clogging of particles in relation to regular sludge. These advantages favor the miniaturization of the system. Authors in [4-6] have established that nanofluids possess variable particle concentrations, including thermal conductivity and adjustable properties to suit various applications and thus significantly improve heat transfer rates. Recently, in the field of heat transfer, studies of nanofluid flow in porous media have garnered much interest as a result of their diverse range of uses in high performance insulation, e.g. grain storage, buildings, packed sphere beds, geothermal systems, solar collectors, and underground spread of pollutants [1, 2, 7-11].

Skin friction is one form of drag, which happens when the fluid appears to shear around the surface of the wall and thereby it affects the energy expenditure. The performance of a forward moving object or fluid flowing through given media improves when the drag is reduced. Authors in [12] established that roughness can cause skin friction inside the pipe or duct or in the boundary layers of the fluid's flow. It was found that systematic roughness can be monitored by knowing which scales of roughness come up with high frictional drag. Most studies have considered a no-slip boundary condition at the solid wall. But in reality, this is not quite correct. For example, numerical experiments have indicated that in composite manufacturing processes and in lubrication approximation, the degree of wall slip becomes more important at wall surfaces, which means that micro and nano processes are used in wall slip [13]. Navier was the first to mention this ailment in 1827 [14]. His model explains that the tangential celerity or

Corresponding author: Wivina Nathan Muyungi

boundary slip velocity (U_s) varies proportionally with the tangential shear stress or shear rate ($\dot{\gamma}$) provided that the amount of slip or proportionality coefficient is constant with regard to the boundary flow conditions. This is called slip length (λ). Slip length is driven by several factors, such as the surface roughness, the strength of the wall-fluid interaction, shear rate, and fluid structure. A non-zero, defined wall slip coefficient would better characterize the state of the wall boundary. Authors in [15-17] established that for a wide variety of materials (e.g. polymers and nanofluids), slip exists on solid surfaces. Such slip is known as the Navier slip. Many studies have been carried out on the Navier slip. Authors in [18] discussed Newtonian fluids flowing in an unsteady through a porous cylindrical pipe with slip conditions. They considered flow behavior for two different cases of small suction and small injection, and established that the magnitude of the axial velocity component is directly proportional to the numerical value of the slip parameter. Further, it has been observed that for small suction the value of the axial velocity component decreases and it increases when there is a small injection. Authors in [19, 20] studied the impact of nanofluid thermal radiation and convection flow due to the cylinder being stretched inside a porous medium, as well as the presence of slip boundary conditions and viscous dissipation. They observed that with a rise in the Eckert number, the thermal slip, the radiation parameters, and the Nusselt number decrease. In addition, with a rise in the velocity, natural convection and slip parameters are enhanced. Studies have established the existence of a close relationship between drag and partial slip parameters. For example, the drag values increase with the increase in the slip parameter [8, 12, 19]. The absolute value of the coefficient of skin friction decreases as heat generation/absorption and thermal radiation increase. Also, the overall stress levels are lowered by the regulated level of partial slip. With more attention to nanomaterials, e.g. nanofluids, it is predicted that there will be an increase in the application of partial slip boundary conditions in the future. Therefore, the slip at the wall surface is important as it can lead to the improvement of the design and operation of many industrial and engineering devices, for example devices for rheometric measurements, material processing, and fluid transportation [21].

In this paper, a mathematical model is developed and used to study the effect of Navier slip and skin friction on nanofluid movement in a porous pipe, which seems to be missing in the literature.

II. MATHEMATICAL MODEL FORMULATION

We consider an unsteady, one dimensional, laminar and incompressible flow through a porous pipe, of Cu and Al_2O_3 as nanoparticles in water-based nanofluids. These nanofluids exhibit a high level of catalytic activity consequently, they improve heat performance, and reduce wall temperature disparities. The two nanofluids are considered to be Newtonian and they are flowing with uniform velocity V. The partial slip condition on the wall of the porous pipe is assumed to hold. According to Newton's law of cooling, the pipe surface exchanges heat with the surrounding environment. The flow problem diagram is expressed in Figure 1.

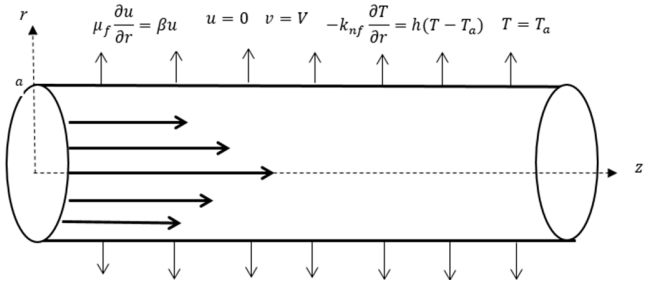

Fig. 1. The schematic flow of the problem.

In Figure 1, the nanofluid temperature is denoted by T, and the velocity in the r-direction is given by u. T_a represents the ambient temperature, μ_f is the dynamic viscosity, k_{nf} is the nanofluid thermal conductivity, (r, θ, z) are the cylindrical polar coordinates, heat transfer coefficient is denoted by h and β represents the Navier slip parameter. The equations governing the flow are:

$$\frac{\partial u}{\partial z} = 0 \quad (1)$$

$$\rho_{nf}\left(\frac{\partial u}{\partial \bar{t}} + V\frac{\partial u}{\partial r}\right) = -\frac{\partial p}{\partial z} + \mu_{nf}\frac{\partial^2 u}{\partial r^2} \quad (2)$$

$$(\rho c_p)_{nf}\left(\frac{\partial T}{\partial \bar{t}} + V\frac{\partial T}{\partial r}\right) = k_{nf}\frac{\partial^2 T}{\partial r^2} + \mu_{nf}\left(\frac{\partial u}{\partial r}\right)^2 \quad (3)$$

where, $\bar{t}$ is the time and p is the nanofluid pressure. The dynamic viscosity of the nanofluid is denoted by μ_{nf}, $(\rho c_p)_{nf}$ is the heat capacity of the nanofluid, and ρ_{nf} represents its density. The nanofluid constants are defined as given in (4):

$$\rho_{nf} = (1-\varphi)\rho_f + \varphi\rho_s$$

$$\alpha_{nf} = \frac{k_{nf}}{(\rho c_p)_{nf}},\ \frac{k_{nf}}{k_f} = \frac{(k_s+2k_f)-2\varphi(k_f-k_s)}{(k_s+2k_f)+\varphi(k_f-k_s)},\ \tau = \frac{(\rho c_p)_s}{(\rho c_p)_f}, \quad (4)$$

$$\mu_{nf} = \frac{\mu_f}{(1-\varphi)^{2.5}},\ (\rho c_p)_{nf} = (1-\varphi)(\rho c_p)_f + \varphi(\rho c_p)_s$$

where ρ_f and ρ_s respectively are the fluid and solid fraction's reference densities, the thermal conductivities of the solid and fluid volume fractions are represented by k_s and k_f, α_{nf} is the thermal diffusivity of the nanofluid, φ is the solid volume fraction of nanoparticles, $(\rho c_p)_s$ is the heat capacity of the solid and the heat capacity of base fluid is $(\rho c_p)_f$.

The initial conditions are given in (5) and the boundary conditions are given in (6) and (7).

$$\mathrm{u(r,0) = 0,\ T(r,0) = T_a},\quad \text{where } 0 \le \mathrm{r} \le \mathrm{a} \quad (5)$$

$$\mu_f \frac{\partial u}{\partial r}(0,\bar{t}), = -\beta u(0,\bar{t}),\qquad T(0,\bar{t}) = T_a \quad (6)$$

$$u(a,\bar{t}) = 0,\quad -k_{nf}\frac{\partial T}{\partial r}T(a,\bar{t}) = h(T(a,\bar{t}) - T_a) \quad (7)$$

TABLE I. NANOPARTICLE AND WATER THERMOPHYSICAL PROPERTIES

Physical properties	Fluid phase (water)	Cu	Al_2O_3
c_p(J/kgK)	4179	385	765
ρ (kg/m^3)	997.1	8933	3970

Source: [22, 23]

The following are introduced as dimensionless variables and parameters:

$$\theta = \frac{T-T_0}{T_a-T_0}, \quad W = \frac{u}{V}, \quad \eta = \frac{r}{a}, \; t = \frac{\bar{t}v_f}{a^2}, \; v_f = \frac{\mu_f}{\rho_f},$$

$$Re = \frac{Va}{v_f}, \; P = \frac{ap}{\mu_f V}, A = -\frac{\partial p}{\partial z}, \; \tau = \frac{(\rho c_p)_s}{(\rho c_p)_f}, \; Z = \frac{z}{a} \quad (8)$$

$$Ec = \frac{V^2}{c_{pf}(T_a-T_0)}, \; Pr = \frac{\mu_f c_{pf}}{k_f}, c_1 = \frac{k_s+2k_f-2\varphi(k_f-k_s)}{k_s+2k_f+\varphi(k_f-k_s)},$$
$$Bi = \frac{ha}{k_f}, \text{ and } \lambda = \frac{\mu_f}{\beta a}$$

Substituting the dimensionless quantities from (8) into (2), (3) and (5) - (7) results into (9) - (13) which form the model equations for this study.

$$\frac{\partial W}{\partial t} = \frac{A}{1-\varphi+\varphi\rho_s/\rho_f} + \frac{1}{(1-\varphi)^{2.5}(1-\varphi+\varphi\rho_s/\rho_f)}\frac{\partial^2 W}{\partial \eta^2} - Re\frac{\partial W}{\partial \eta} \quad (9)$$

$$\frac{\partial \theta}{\partial t} = c_1 \frac{1}{Pr(1-\varphi+\varphi\tau)}\frac{\partial^2 \theta}{\partial \eta^2} + \frac{Ec}{(1-\varphi)^{2.5}(1-\varphi+\varphi\tau)}\left(\frac{\partial W}{\partial \eta}\right)^2 - Re\frac{\partial \theta}{\partial \eta} \quad (10)$$

$$W(\eta,0) = 0, \; \theta(\eta,0) = 0 \quad (11)$$

$$\frac{\partial W}{\partial \eta}(0,t) = -\frac{\beta a}{\mu_f}W(0,t), \quad \theta(0,t) = 0 \quad (12)$$

$$W(1,t) = 0, \; \frac{\partial \theta}{\partial \eta}(1,t) = -mBi\theta(1,t) \quad (13)$$

where Re is the Raynolds number, A is the parameter for pressure gradient, Pr denotes the Prandtl number and Ec represents the Eckert number. The base fluid and the thermophysical properties of the nanoparticles can be used to derive the values of the parameters c_1 and τ.

The skin friction (C_f) and the Nusselt number (Nu) are crucial for this type of study. They are defined as:

$$C_f = \frac{a\tau_w}{\mu_0 V}, \quad Nu = \frac{aq_w}{k_f(T_w-T_0)} \quad (14)$$

where q_w is the heat flux at the pipe wall and τ_w is the wall shear stress given by:

$$\tau_w = -\mu_{nf}\frac{\partial u}{\partial r}\Big|_{r=a}, \quad q_w = -k_{nf}\frac{\partial T}{\partial r}\Big|_{r=a} \quad (15)$$

Substituting τ_w and q_w from (15) into (14) and using the dimensionless variables with manipulations results to:

$$C_f = -\frac{1}{(1-\varphi)^{2.5}}\frac{\partial W}{\partial \eta} \quad \text{at } \eta = 1 \quad (16)$$

$$Nu = c_1\frac{\partial \theta}{\partial \eta}$$

III. NUMERICAL PROCEDURE

The method of lines [24] is a semi-discretization finite difference approach for numerically solving a nonlinear Initial Boundary Value Problem (IBVP). We divide the solution region into equal rectangles or meshes. Each mesh point specifies the point's position in terms of t and ΔW or $\Delta\eta$ .The horizontal axis represents spatial variables, while the vertical axis represents time variables in this rectangular mesh grid. The method is used to discretize (9) to (13) which results in (21)-(24). Then, the discretization of the partial differential equations (8) and (9) using second order central finite differences results in ordinary differential equations (21) and (22).

$$\frac{dW}{dt} = \frac{A}{1-\varphi+\varphi\rho_s/\rho_f} +$$

$$\frac{1}{(1-\varphi)^{2.5}(1-\varphi+\varphi\rho_s/\rho_f)}\left(\frac{W_{i+1}-2W_i+W_{i-1}}{\Delta\eta^2}\right) - Re\left(\frac{W_{i+1}-W_{i-1}}{2\Delta\eta}\right) \quad (17)$$

$$\frac{d\theta}{dt} = c_1\frac{1}{\Pr(1-\varphi+\varphi\tau)}\left(\frac{\theta_{i+1}-2\theta_i+\theta_{i-1}}{\Delta\eta^2}\right) +$$

$$\frac{E_C}{(1-\varphi)^{2.5}(1-\varphi+\varphi\tau)}\left(\frac{W_{i+1}-W_{i-1}}{2\Delta\eta}\right)^2 - Re\left(\frac{\theta_{i+1}-\theta_{i-1}}{2\Delta\eta}\right) \quad (18)$$

where $W_i(t)$ and $\theta_i(t)$ are the approximations of $W(\eta_i,t)$ and $\theta(\eta_i,t)$.

With initial conditions (11) we get (23) and boundary conditions (12) and (13) result in (24).

$$W_i(0) = \theta_i(0) = 0, \; 1 \le i \le N+1 \quad (19)$$

$$W_i = \frac{-\lambda W_2}{\Delta\eta-\lambda}, \; \varphi_1 = 0, \; W_{N+1} = 1, \; \theta_{N+1} = \varphi_N(1-mBi\Delta\eta) \quad (20)$$

The system of nonlinear ordinary differential equations (17) and (18) with known initial condition (19) and boundary conditions (20) has been solved in Matlab.

IV. RESULTS AND DISCUSSION

Water-based nanofluids of two types, Cu and Al_2O_3, are considered in this study, while the Prandtl number is fixed at 6.2, and the effect of the slip parameter (λ), solid volume fraction (φ), Reynold number (Re), Biot number (Bi), and pressure gradient (A) on the velocity profile and temperature profile are examined. Figure 2 shows that the nanofluid velocity profile of Al_2O_3 is higher than that of Cu and this may be attributed to the specific heat capacity of Al_2O_3 being higher than that of Cu. Also, the density of Copper is higher than that of Alumina.

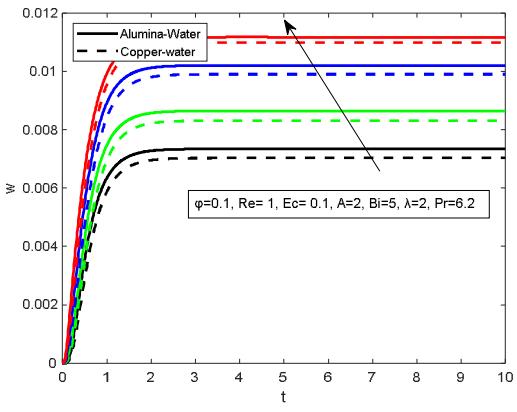

Fig. 2. Copper and alumina nanofluid velocity profile.

Figure 3 depicts the effect of nanoparticle fraction in velocity, demonstrating that as the nanoparticle fraction (φ) increases, velocity decreases at the wall compared to the center

of the pipe. This may be due to the fact that the increase of nanoparticle regulates temperature of the fluid and causes the thermal boundary layer's viscosity to increase. Also this could be due to the density of the nanofluid. An increase in *Re* leads to a decline in velocity and this may be is caused by the uniform flow of nanofluid as revealed in Figure 4. Figure 5 displays that velocity decreases with increase in λ. This effect may be due to the nanofluid sticking at the wall which lowers the velocity and also due to the high viscosity of the fluid.

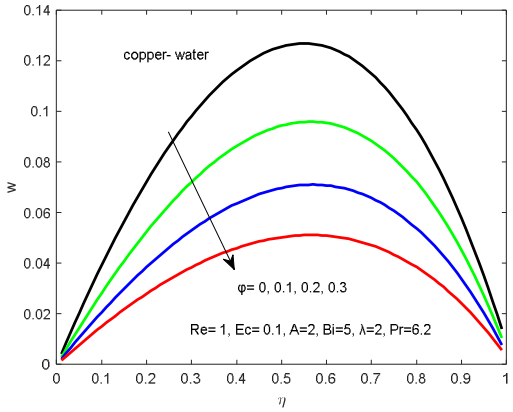

Fig. 3. Effect of increasing φ on velocity profiles.

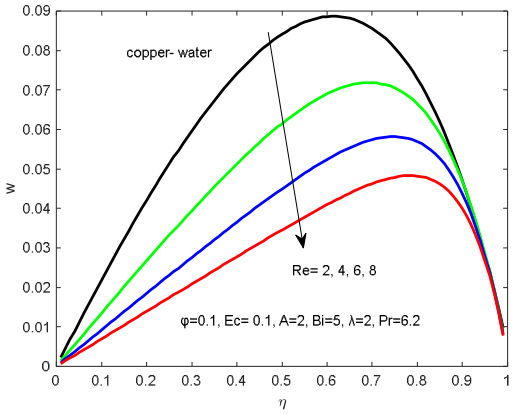

Fig. 4. Effect of increasing *Re* on velocity profiles.

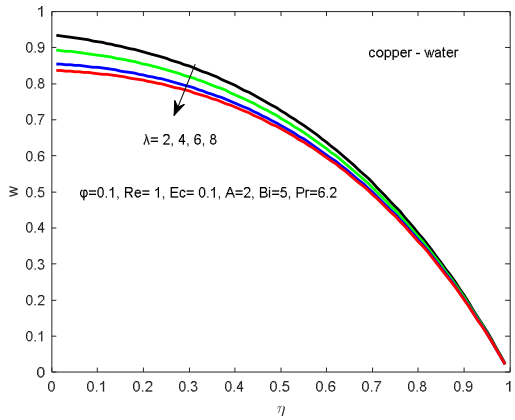

Fig. 5. Effect of increasing λ on velocity profiles.

Figures 6-9 illustrate the temperature profiles of the nanofluids in the pipe and the impact of various factors on the fluid flow system. The temperature profile decreases as the φ increases as shown in Figure 6, maybe due to the increase of the density of the nanofluid. Figure 7 illustrates the temperature decrease due to the increase of *Re*. When it reaches the wall of the pipe the temperature starts to rise due to the slippery walls.

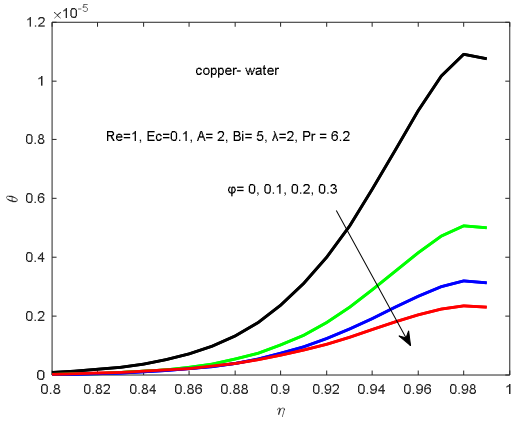

Fig. 6. Effect of increasing φ on temperature profile.

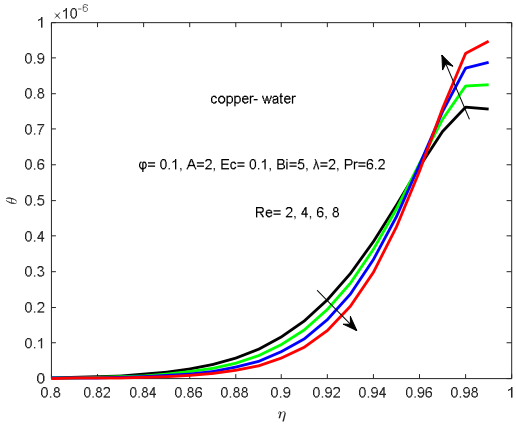

Fig. 7. Effect of increasing *Re* on temperature profile.

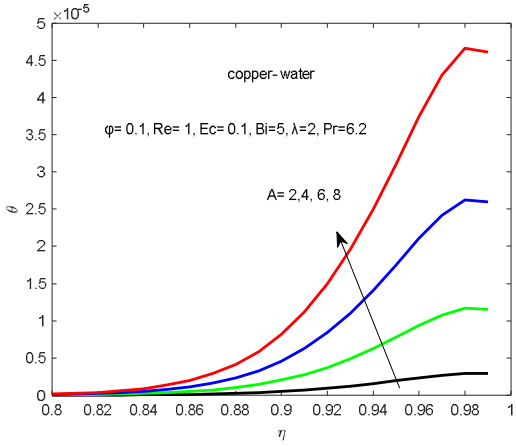

Fig. 8. Effect of increasing *A* on temperature profile.

In Figure 8, as the pressure gradient (A) increases, temperature also increases since the viscosity is reduced. In Figure 9, the increase in Bi is associated with a reduction in temperature. This could be attributed to the convective cooling at the walls which means that there is heat loss through the wall. As demonstrated in Figure 10, copper-water nanofluid skin friction is higher than alumina-water nanofluid skin friction. This difference may be caused by the specific heat capacity of alumina which is lower than that of copper. Also alumina-water has a lower velocity gradient near the channel walls than Cu-water, hence this is to be expected.

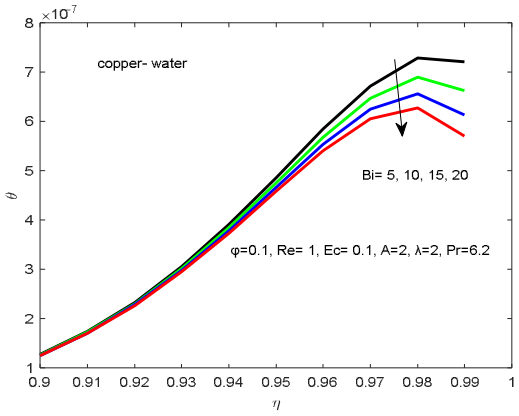

Fig. 9. Effect of increasing Bi on temperature profile.

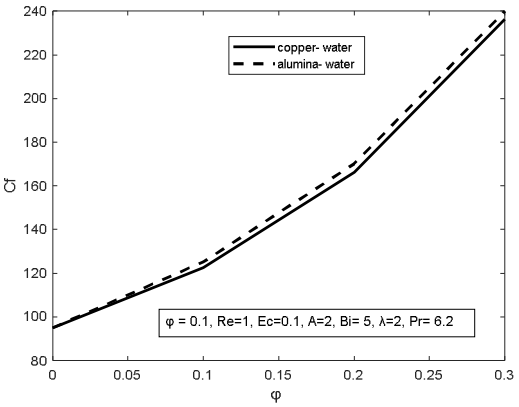

Fig. 10. Effect of increasing φ on the skin friction of Cu and Al_2O_3 nanofluids.

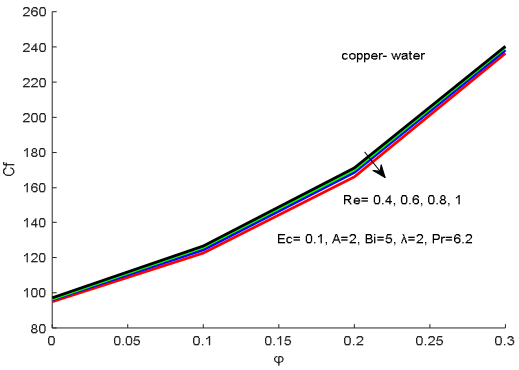

Fig. 11. Effect of increasing *Re* on skin friction.

In Figure 11, the decrease of skin friction with the increase of *Re* may be due to the slip parameter. This result is inconsistent with the results obtained in [5-7]. In Figure 12, we see that pressure gradient is inversely proportional to skin friction because the kinetic energy of the fluid is used to overcome the friction of the surface during the flow. This result is consistent with the results obtained in [5]. In Figure 13, by means of an increase in *Re*, the Nusselt number also increases, since during the flow, there is more heat which is produced due to the increase of speed. The viscosity is also reduced.

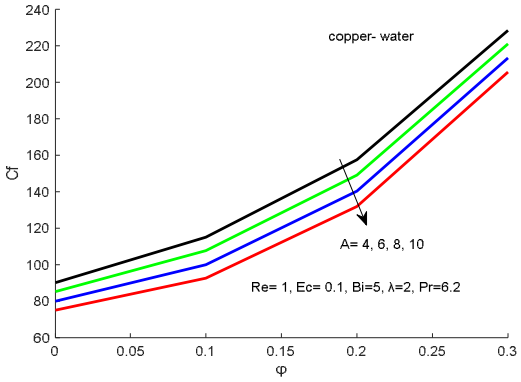

Fig. 12. Effect of increase in *A* on skin friction.

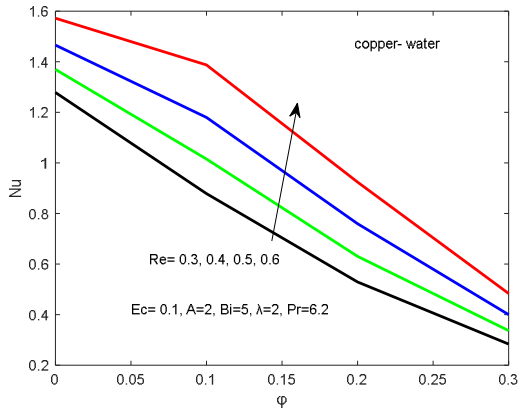

Fig. 13. Effect of increasing *Re* in Nusselt number.

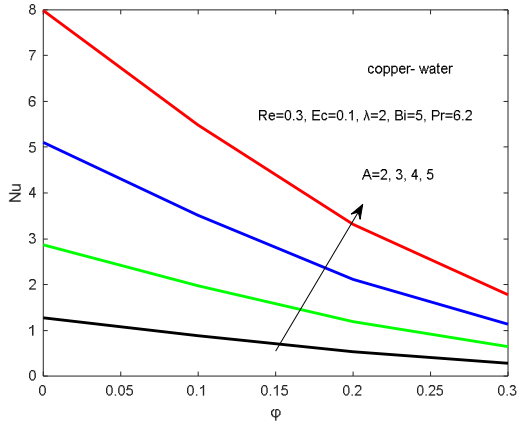

Fig. 14. Effect of increasing *A* on Nusselt number.

In Figure 14, we observe that the Nusselt number increases with the increase of pressure gradient since there is more force exerted which cause reduction in viscosity during nanofluid flow. In Figure 15, the Nusselt number also increases when the Biot number increases, maybe due to the reduction in viscosity since the fluid has a higher thermal conductivity. The decrease of Nusselt number with increase in slip parameter because of the convective cooling at the wall is presented in Figure 16.

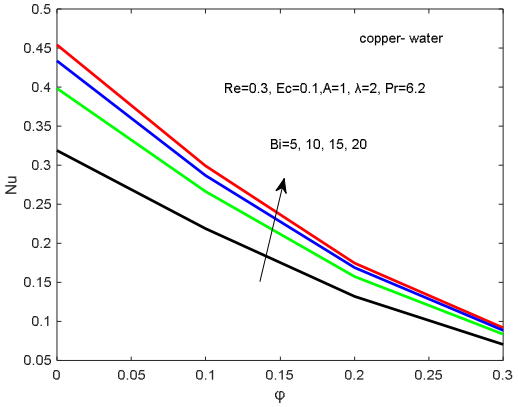

Fig. 15. Effect of increasing Bi on Nusselt number.

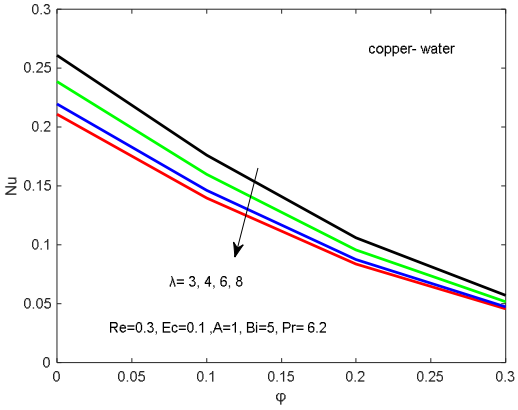

Fig. 16. Effect of increasing λ on Nusselt number

V. CONCLUSION

The effect of Navier slip and skin friction of nanofluid flow in a porous pipe have been investigated in this study. The simplified system of ordinary differential equations is numerically solved with the line method. The following is a list of the findings of the current study:

- The velocity and temperature is enhanced by the Reynolds number. Navier slip parameter causes a decrease of velocity and a rise in Biot number coincided with a drop in temperature.
- The temperature and velocity of copper-water nanofluid rises faster than that of alumina-water nanofluid.
- Skin friction is retarded by increasing the Reynolds number, so we need to increase the volume of nanoparticles in the base fluid to overcome the increased skin friction. An increase of Reynolds number or Biot number causes the heat transfer at the wall to increase and the opposite for slip parameter. Therefore, near the wall, Navier slip reduces friction of the porous pipes, such that the more heat is transferred from the system by non-linear radiation. In a linear thermal distribution, the energy transfer coefficient is higher than in a non-linear thermal distribution.

NOMENCLATURE

ρ_{nf}	Nanofluid density (kg.m^{-3})
μ	Dynamic viscosity (kg/m.s)
μ_k	Kinematic viscosity (m^2/s)
k_{nf}	Nanofluid thermal conductivity (W/m.K)
φ	Concentration of nanoparticles
c_p	Specific heat capacity (J/kg.K)
β	Navier slip parameter
T	Nanofluid temperature (K)
T_a	Ambient temperature (K)
Bi	Local Biot number
Pr	Prandtl number
Ec	Eckert number
A	Dimensionless pressure gradient
C_f	Skin friction coefficient
Nu	Nusselt number
P	Pressure

ACKNOWLEDGMENT

The authors acknowledge the support of Nelson Mandela African Institution of Science and Technology.

REFERENCES

[1] M. E. Erdogan and C. E. Imrak, "On the flow in a uniformly porous pipe," *International Journal of Non-Linear Mechanics*, vol. 43, no. 4, pp. 292–301, Feb. 2008, https://doi.org/10.1016/j.ijnonlinmec.2007.12.006.

[2] A. Kasaeian *et al.*, "Nanofluid flow and heat transfer in porous media: A review of the latest developments," *International Journal of Heat and Mass Transfer*, vol. 107, pp. 778–791, Dec. 2017, https://doi.org/10.1016/j.ijheatmasstransfer.2016.11.074.

[3] S. U. S. Choi and J. A. Eastman, "Enhancing thermal conductivity of fluids with nanoparticles," in *International Mechanical Engineering Congress and Exhibition*, San Francisco, CA, USA, Nov. 1995.

[4] N. A. Rawi, A. R. Mohd Kasim, Z. Mat Isa, A. Mangi, and S. Shafie, "G-jitter effects on the mixed convection flow of nanofluid past an inclined stretching sheet," *Frontiers in Heat and Mass Transfer*, vol. 8, 2017, Art. no. 12, https://doi.org/10.5098/hmt.8.12.

[5] M. H. Mkwizu, O. D. Makinde, and Y. Nkansah-Gyekye, "Effects of Navier Slip and Wall Permeability on Entropy Generation in Unsteady Generalized Couette Flow of Nanofluids With Convective Cooling," *UPB Scientific Bulletin*, vol. 77, no. 4, pp. 201–216, 2015.

[6] M. Danikas, "Breakdown in Nanofluids: A Short Review on Experimental Results and Related Mechanisms," *Engineering, Technology & Applied Science Research*, vol. 8, no. 5, pp. 3300–3309, Oct. 2018, https://doi.org/10.48084/etasr.2136.

[7] S. A. Khamis, "Analysis and Simulation of Nanofluid Flow and Heat Transfer in a Porous Pipe," Ph.D. dissertation, The Nelson Mandela AFrican Institution of Science and Technology, Arusha, Tanzania, 2016.

[8] W. N. Mutuku-Njane and O. D. Makinde, "Combined Effect of Buoyancy Force and Navier Slip on MHD Flow of a Nanofluid over a Convectively Heated Vertical Porous Plate," *The Scientific World Journal*, vol. 2013, Oct. 2013, Art. no. e725643, https://doi.org/10.1155/2013/725643.

[9] M. Elashmawy, A. A. A. A. Al-Rashed, L. Kolsi, I. Badawy, N. B. Ali, and S. S. Ali, "Heat Transfer and Fluid Flow in Naturally Ventilated Greenhouses," *Engineering, Technology & Applied Science Research*,

vol. 7, no. 4, pp. 1850–1854, Aug. 2017, https://doi.org/10.48084/etasr.1269.

[10] A. Latreche and M. Djezzar, "Numerical Study of Natural Convective Heat and Mass Transfer in an Inclined Porous Media," *Engineering, Technology & Applied Science Research*, vol. 8, no. 4, pp. 3223–3227, Aug. 2018, https://doi.org/10.48084/etasr.2179.

[11] H. A. Fakhim, "An Investigation of the Effect of Different Nanofluids in a Solar Collector," *Engineering, Technology & Applied Science Research*, vol. 7, no. 4, pp. 1741–1745, Aug. 2017, https://doi.org/10.48084/etasr.1283.

[12] K. A. Flack, M. P. Schultz, J. M. Barros, and Y. C. Kim, "Skin-friction behavior in the transitionally-rough regime," *International Journal of Heat and Fluid Flow*, vol. 61, pp. 21–30, Jul. 2016, https://doi.org/10.1016/j.ijheatfluidflow.2016.05.008.

[13] J. Eijkel, "Liquid slip in micro- and nanofluidics: recent research and its possible implications," *Lab on a Chip*, vol. 7, no. 3, pp. 299–301, Mar. 2007, https://doi.org/10.1039/b700364c.

[14] C. Y. Wang and C.-O. Ng, "Slip flow due to a stretching cylinder," *International Journal of Non-Linear Mechanics*, vol. 46, no. 9, pp. 1191–1194, Aug. 2011, https://doi.org/10.1016/j.ijnonlinmec.2011.05.014.

[15] T. Sochi, "Slip at Fluid-Solid Interface," *Polymer Reviews*, vol. 51, no. 4, pp. 309–340, Jul. 2011, https://doi.org/10.1080/15583724.2011.615961.

[16] K. A. Nair and A. Sameen, "Experimental Study of Slip Flow at the Fluid-porous Interface in a Boundary Layer Flow," *Procedia IUTAM*, vol. 15, pp. 293–299, Jan. 2015, https://doi.org/10.1016/j.piutam.2015.04.041.

[17] S. Hussain, A. Aziz, T. Aziz, and C. M. Khalique, "Slip Flow and Heat Transfer of Nanofluids over a Porous Plate Embedded in a Porous Medium with Temperature Dependent Viscosity and Thermal Conductivity," *Applied Sciences*, vol. 6, no. 12, Dec. 2016, Art. no. 376, https://doi.org/10.3390/app6120376.

[18] K. Bhatti, Z. Bano, and A. M. Siddiqui, "Unsteady Stokes Flow through Porous Channel with Periodic Suction and Injection with Slip Conditions," *European Journal of Pure and Applied Mathematics*, vol. 11, no. 4, pp. 937–945, Oct. 2018, https://doi.org/10.29020/nybg.ejpam.v11i4.3309.

[19] A. K. Pandey and M. Kumar, "Natural convection and thermal radiation influence on nanofluid flow over a stretching cylinder in a porous medium with viscous dissipation," *Alexandria Engineering Journal*, vol. 56, no. 1, pp. 55–62, Nov. 2017, https://doi.org/10.1016/j.aej.2016.08.035.

[20] A. K. Pandey and M. Kumar, "Boundary layer flow and heat transfer analysis on Cu-water nanofluid flow over a stretching cylinder with slip," *Alexandria Engineering Journal*, vol. 56, no. 4, pp. 671–677, Sep. 2017, https://doi.org/10.1016/j.aej.2017.01.017.

[21] D. M. Kalyon, "Apparent slip and viscoplasticity of concentrated suspensions," *Journal of Rheology*, vol. 49, no. 3, pp. 621–640, Feb. 2005, https://doi.org/10.1122/1.1879043.

[22] J. Wang, J. Zhu, X. Zhang, and Y. Chen, "Heat transfer and pressure drop of nanofluids containing carbon nanotubes in laminar flows," *Experimental Thermal and Fluid Science*, vol. 44, pp. 716–721, Jan. 2013, https://doi.org/10.1016/j.expthermflusci.2012.09.013.

[23] H. F. Oztop and E. Abu-Nada, "Numerical study of natural convection in partially heated rectangular enclosures filled with nanofluids," *International Journal of Heat and Fluid Flow*, vol. 29, no. 5, pp. 1326–1336, Jul. 2008, https://doi.org/10.1016/j.ijheatfluidflow.2008.04.009.

[24] K. W. Morton and D. F. Mayers, *Numerical Solution of Partial Differential Equations*. New York, NY, USA: Cambridge University Press, 2005.